Tracking the epicenter and the tsunami origin with GPS ionosphere observation

Ho-Fang Tsai[1,2], Jann-Yenq Liu[3,4,5], Chien-Hung Lin[6], and Chia-Hung Chen[7]

[1]*Taiwan Analysis Center for COSMIC (TACC), Central Weather Bureau, Taipei, Taiwan*
[2]*GPS Scientific Application Research Center (GPS-ARC), National Central University, Jhongli City, Taiwan*
[3]*Institute of Space Science, National Central University, Jhongli City, Taiwan*
[4]*Center for Space and Remote Sensing Research, National Central University, Jhongli City, Taiwan*
[5]*National Space Organization, Hsinchu, Taiwan*
[6]*Department of Earth Science, National Cheng Kung University, Tainan, Taiwan*
[7]*Department of Geophysics, Kyoto University, Kyoto, Japan*

(Received April 8, 2011; Revised June 14, 2011; Accepted June 15, 2011; Online published September 27, 2011)

The global positioning system (GPS) can be used to monitor the seismic perturbation induced by the 2011 off the Pacific coast of Tohoku Earthquake (magnitude 9.0), Japan, on March 11, 2011, and to trace the tsunami across the Pacific Ocean by measuring the changes in the ionospheric total electron content (TEC). We estimate the vertical and horizontal mean speeds of the seismic and tsunami waves using the time and distance of the TEC perturbation, and then, taking into account those determined speeds, trace back to the epicenter and the tsunami origin by applying a 3-dimensional spherical model. The results show that both the tracked epicenter and the tsunami origin are quite close to the epicenter reported by the USGS, with a mean horizontal propagation speed of 2.3 km/s after the earthquake and about 210 m/s after the tsunami. This consistency confirms that the perturbation sources in the ionosphere are due to the earthquake. This implies that the GPS-TEC measurements have the potential to be part of a lower cost, ground-based, tsunami monitoring system.
Key words: GPS, ionospheric total electron content, TEC, tsunami, 2011 Tohoku earthquake.

1. Introduction

Since the atmospheric density decreases almost exponentially with altitude, energy conservation implies that the pulse amplitude increases upwards as it propagates into the atmosphere (Calais and Minster, 1995). In the past, many seismo-ionosphere observations based on ionosondes, high-frequency Doppler sounding systems and ground-based global positioning system (GPS) receivers have been published (Davies and Baker, 1965; Leonard and Barnes, 1965; Row, 1966; Yuen *et al.*, 1969; Tanaka *et al.*, 1984; Calais and Minster, 1995; Afraimovich *et al.*, 2001; Ducic *et al.*, 2003; Artru *et al.*, 2004; Liu *et al.*, 2005, 2011). On the other hand, tsunami waves propagating across long distances in the open ocean can also induce atmospheric gravity waves by dynamic coupling at the surface (Najita *et al.*, 1974; Okal *et al.*, 1999; Artru *et al.*, 2005; Gower, 2005; Blewitt *et al.*, 2006; Liu *et al.*, 2006; Occhipinti *et al.*, 2008; Galvan *et al.*, 2011). The seismic and tsunamigenic signatures in the ionosphere are referred to as seismo-traveling ionospheric disturbances (STIDs) (Liu *et al.*, 2011).

The U.S. Geological Survey (USGS) reported that the origin time of the magnitude 9.0 earthquake was at 05:46:23 UTC; while the epicenter was located at 38.322°N, 142.369°E off the east coast of the Tohoku area, Japan (USGS, 2011). Displacement of the adjacent seabed generated gigantic tsunami waves damaging many coastal communities around the Tohoku area. In this paper, we use data from a total of 17 ground-based GPS stations in the GEONET network in Japan, the IGS network and the Taiwan GPS network to detect the ionospheric perturbation induced by the 2011 Tohoku earthquake and the subsequent tsunami, and then trace their origins using a 3-dimensional spherical model.

2. Observation of the Earthquake

In order to study the ionospheric signature of the earthquake, we process the GPS data from the continuous GEONET in Japan (4 stations designated as 0020, 0047, 0119 and 0232), the IGS (7 stations named ccj2, cusv, daej, guam, mizu, pimo and shao) and Taiwan GPS network (2 stations named aknd and alis). The vertical total electron content (TEC) in the ionosphere derived from the GPS data is based on the method of Liu *et al.* (1996), assuming an ionospheric height of 325 km. Figure 1 shows the variation in TEC (dTEC) for 29 GPS receiver-satellite pairs. Compared with the quiet behavior before the earthquake, the sudden disturbances in TEC are taken to be due to seismic perturbations triggered by the 2011 Tohoku earthquake. After the sudden disturbances with periods of the order of minutes, some quasi-sinusoidal waves may appear with longer periods, e.g. the pair ‘ccj2#15’ after 6.5 hours.

Based on the method of Liu *et al.* (2006), the times at the maximum dTEC amplitude for those 29 pairs and their

doi:10.5047/eps.2011.06.024

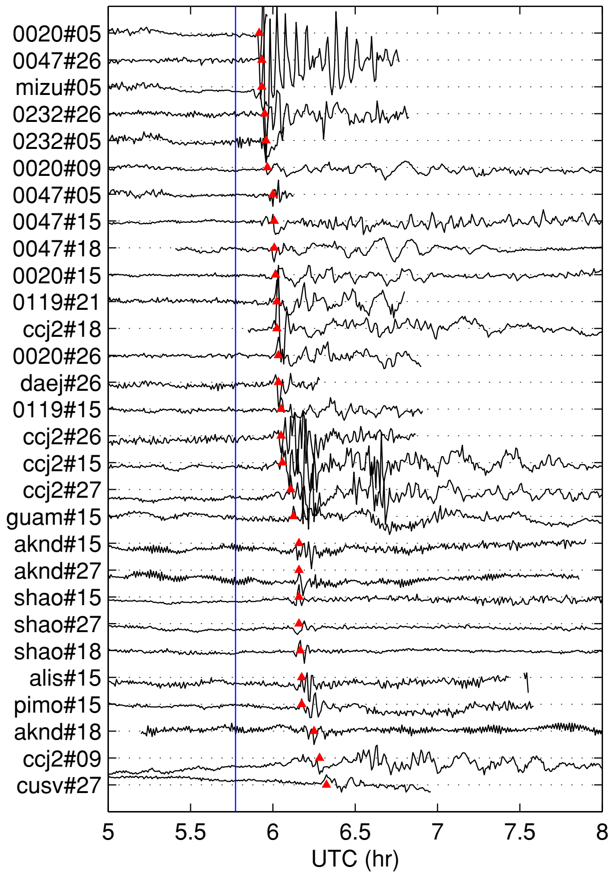

Fig. 1. Time-differencing TEC from 29 GPS receiver-satellite pairs. The vertical axis denotes each pair with four alphanumeric (site name) and two numbers (GPS PRN number), divided by a hatch sign. Each curve denotes dTEC between every two adjacent measurements for 30-s sampling. The grid lines indicate the amplitude of dTEC (0.4 TECU for each grid; 1 TECU $= 10^{16}$ m^{-3}). The blue line and the red triangles indicate the origin time of the earthquake and the maximum dTEC, respectively.

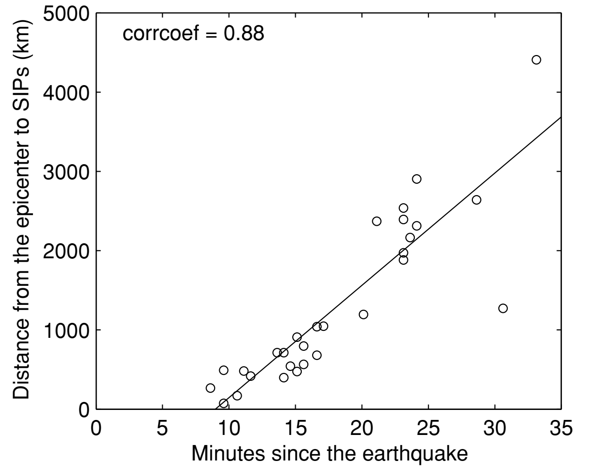

Fig. 2. The correlation between the 29 times of the maximum dTEC and their corresponding distances from the epicenter (reported by the USGS) to the SIPs, denoted by circles. The slanted line indicates the regression line of the data.

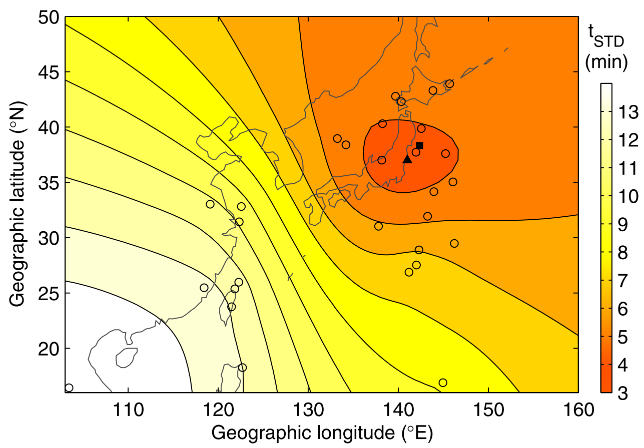

Fig. 3. Contour of STD of the travel times estimated by the 3-dimensional spherical model. The circles indicate the location of SIPs; the triangle indicates the location of the minimum STD value; the square indicates the epicenter reported by the USGS.

corresponding distance from the epicenter can be plotted as Fig. 2. Statistical analysis shows that the correlation coefficient for the 29 records is 0.88. The linear regression shows that the nearest sub-ionospheric point (SIP) is not disturbed until 9 min after the earthquake, i.e. the seismic signal propagates with a vertical mean speed of 0.6 km/s (= 325 km/9 min; as an acoustic gravity wave speed) to the nearest ionospheric point (IP) above the epicenter. The slope of the regression line implies a mean horizontal speed of 2.3 km/s along the surface, which is within the range of Rayleigh wave speeds.

Taking the speeds estimated above, the time and the location of the 29 SIPs, we try to estimate the location of the epicenter in a 3-dimensional spherical model in a ray-tracing sense. The origin time of the earthquake and the location of the epicenter are omitted from the system at the beginning. The model calculates the travel time of the seismic waves propagating along the surface from a trial point on the Earth's surface to the SIP and then vertically propagating to the IP for each receiver-satellite pair. The model then estimates the standard deviation (STD) of 29 travel times until the minimum STD value is located on the map, which point will be the optimal time and location estimated by the model. Figure 3 shows the trial result from the model where the optimal location (triangle mark) is 183 km distant from the reported epicenter (square mark). The optimal time is 05:46:12 UTC ± 3.5 minutes, which is quite close to the reported time 05:46:23 UTC.

3. Observation of the Tsunami

According to the different characteristics of the dTEC disturbance by the tsunami, we consider another set of time-series dTEC having periods of the order of 10-min and relocate the local maximum dTEC for 27 receiver-satellite pairs from the GEONET (3 sites known as 0020, 0047 and 0232) and the IGS (6 sites named albh, ccj2, daej, dhlg, guam, mcil, pimo and tskb) as shown in Fig. 4. Similar to Fig. 2, the linear regression can also apply on this new data set as shown in Fig. 5. Unlike Fig. 2, the regression line goes through the origin for the tsunami although the correlation coefficient 0.99 is higher. The slope of the regression line indicates the mean speed of the horizontal propagating waves to be 210 m/s (subsonic speed). As the atmo-

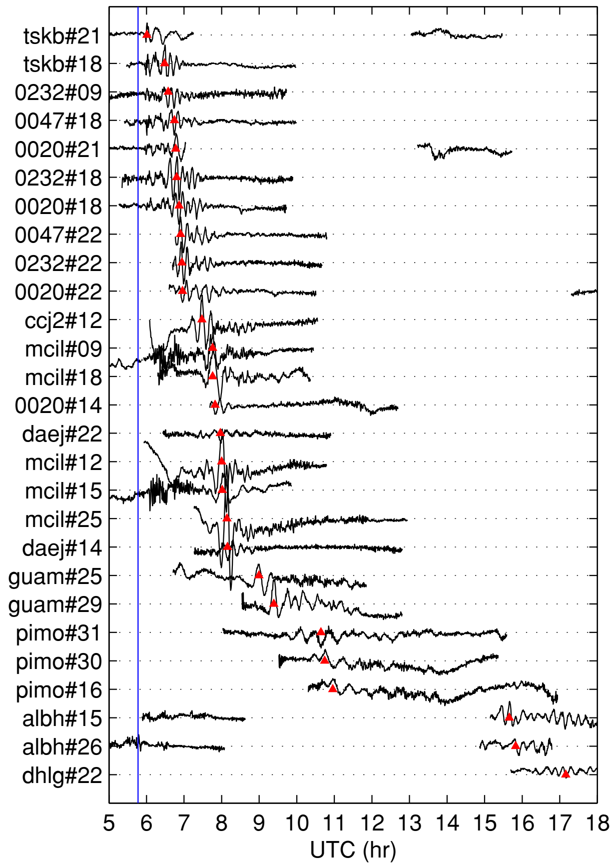

Fig. 4. Same as Fig. 1 but focusing on dTEC with 10-min class periods.

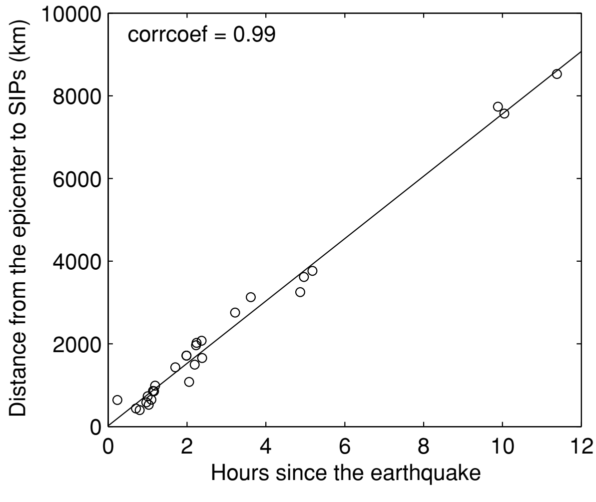

Fig. 5. Same as Fig. 2 but for the tsunami.

spheric medium can hardly change significantly between the earthquake and the tsunami, the mean speed of the vertical propagating waves should be around 600 m/s, but not infinity. The time spread and non-uniform speeds regarding tsunamis may be the reason for the 9 min bias from the origin. We again estimate the optimal time and the location of the tsunami origin using the previous model assuming a 600 m/s vertical speed (Fig. 6) and obtain the tsunami source, 195 km northwest of the real epicenter. The estimated tsunami occurrence time is 05:33:36 UTC $\pm$ 14.8

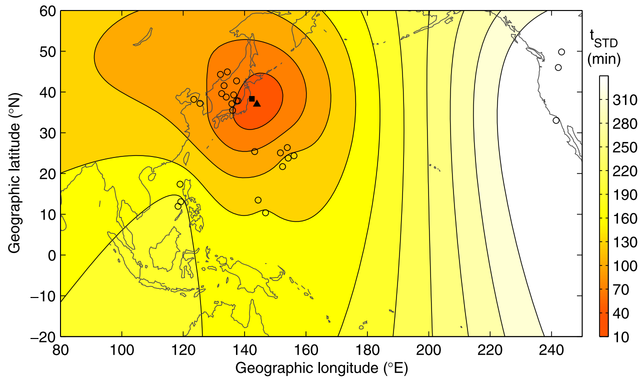

Fig. 6. Same as Fig. 3 but for tsunami.

minutes, which is ahead of the real occurrence time by 13 minutes, within the range of the minimum standard deviation.

4. Summary

The seismic ionosphere technique based on a network of GPS receiver-satellite pairs can distinguish the seismic perturbation and tsunami-induced waves in the time-variant TEC difference, where the former tends to a larger amplitude and shorter wavelength whereas the latter tends to a smaller amplitude and longer wavelength as shown in Figs. 1 and 4. For the 2011 Tohoku earthquake, the mean horizontal and vertical speeds of the seismic propagating waves are estimated to be 2.3 km/s; and for the subsequent tsunami, the mean horizontal speed is 210 m/s. Applying a 3-dimensional ray-tracing model and these speeds, we predict the optimal time and location of the earthquake and the tsunami, which confirms that the TEC disturbance can be traced back to their origins.

Acknowledgments. This research was partially supported by National Science Council and National Space Organization in Taiwan under grant NSC 98-2116-M-008-006-MY3 and NSPO-S-100011, respectively. GPS observation files used in this work were provided by the Geospatial Information Authority of Japan (GSI), Central Weather Bureau of Taiwan (CWB), and International GNSS Service (IGS).

References

Afraimovich, E. L., N. P. Perevalova, A. V. Plotnikov, and A. M. Uraloy, The shock-acoustic waves generated by earthquakes, *Ann. Geophys.*, **19**, 395–409, 2001.

Artru, J., T. Farges, and P. Lognonné, Acoustic waves generated from seismic surface waves: Propagation properties determined from Doppler sounding observations and normal-mode modeling, *Geophys. J. Int.*, **158**, 1067–1077, 2004.

Artru, J., V. Ducic, H. Kanamori, P. Lognonné, and M. Murakami, Ionospheric detection of gravity waves induced by tsunamis, *Geophys. J. Int.*, **160**, 840–848, 2005.

Blewitt, G., C. Kreemer, W. C. Hammond, H.-P. Plag, S. Stein, and E. Okal, Rapid determination of earthquake magnitude using GPS for tsunami warning systems, *Geophys. Res. Lett.*, **33**, L11309, doi:10.1029/2006GL026145, 2006.

Calais, E. and J. B. Minster, GPS detection of ionospheric perturbations following the January 17, 1994, Northridge earthquakes, *Geophys. Res. Lett.*, **22**, 1045–1048, 1995.

Davis, K. and D. M. Baker, Ionospheric effects observed around the time of the Alaskan earthquake of March 28, 1964, *J. Geophys. Res.*, **22**, 2251–2253, 1965.

Ducic, V., J. Artru, and P. Lognonné, Ionospheric remote sensing of the

Denali earthquake Rayleigh surface waves, *Geophys. Res. Lett.*, **30**(18), doi:10.1029/2003GL017812, 2003.

Galvan, D. A., A. Komjathy, M. P. Hickey, and A. J. Mannucci, The 2009 Samoa and 2010 Chile tsunamis as observed in the ionosphere using GPS total electron content, *J. Geophys. Res.*, **116**, A06318, doi:10.1029/2010JA016204, 2011.

Gower, J., Jason 1 detects the 26 December 2004 tsunami, *Eos*, **86**, 37–38, 2005.

Leonard, R. S. and R. A. Barnes, Jr., Observation of ionospheric disturbances following the Alaska earthquake, *J. Geophys. Res.*, **70**, 1250–1253, 1965.

Liu, J. Y., H. F. Tsai, and T. K. Jung, Total electron content obtained by using the global positioning system, *Terr. Atmos. Ocean. Sci.*, **7**(1), 107–117, 1996.

Liu, J. Y., Y. B. Tsai, S. W. Chen, C. P. Lee, Y. C. Chen, H. Y. Yen, W. Y. Chang, and C. Liu, Giant ionospheric disturbances excited by the M9.3 Sumatra earthquake of 26 December 2004, *Geophys. Res. Lett.*, **33**, L02103, doi:10.1029/2005GL023963, 2005.

Liu, J. Y., Y. B. Tsai, K. F. Ma, Y. I. Chen, H. F. Tsai, C. H. Lin, M. Kamogawa, and C. P. Lee, Ionospheric GPS total electron content (TEC) disturbances triggered by the 26 December 2004 Indian Ocean tsunami, *J. Geophys. Res.*, **111**, A05303, doi:10.1029/2005JA011200, 2006.

Liu, J. Y., C. H. Chen, C. H. Lin, H. F. Tsai, C. H. Chen, and M. Kamogawa, Ionospheric disturbances triggered by the 11 March 2011 M9.0 Tohoku earthquake, *J. Geophys. Res.*, **116**, A06319, doi:10.1029/2011JA016761, 2011.

Najita, K., P. F. Weaver, and P. C. Yuen, A tsunami warning system using an ionospheric technique, *Proc. IEEE*, **62**, 563–567, 1974.

Occhipinti, G., A. Komjathy, and P. Lognonné, Tsunami detection by GPS, *GPS World*, **19**(2), 51–57, 2008.

Okal, E. A., A. Piatanesi, and P. Heinrich, On the possible detection of tsunamis by a monitoring of the ionosphere, *J. Geophys. Res.*, **104**(B1), 599–615, 1999.

Row, R. V., Evidence of long-period acoustic-gravity waves launched into the F-region by the Alaskan earthquake of March 28, 1964, *J. Geophys. Res.*, **71**, 343–345, 1966.

Tanaka, T., T. Ichinose, T. Okuzawa, T. Shibata, Y. Sato, C. Nagasawa, and T. Ogawa, HF-Doppler observations of acoustic waves excited by the Urakawa-Oki earthquake on 21 March 1982, *J. Atmos. Terr. Phys.*, **46**, 233–245, 1984.

USGS, Magnitude 9.0—Near the east coast of Honshu, Japan, http://earthquake.usgs.gov/earthquakes/eqinthenews/2011/usc0001xgp/ (last access April 7, 2011), 2011.

Yuen, P. C., P. F. Weaver, R. K. Suzuki, and A. S. Furumoto, Continuous traveling coupling between seismic waves and the ionosphere evident in May 1968 Japan earthquake data, *J. Geophys. Res.*, **74**, 2256–22674, 1969.

H.-F. Tsai (e-mail: hftsai@cwb.gov.tw), J.-Y. Liu, C.-H. Lin, and C.-H. Chen